Talk at the 9e Session d'Etudes Biennale de Physique Nucléaire, Aussois 9-13 Mars 1987

RELATIVISTIC APPROACH TO NUCLEAR STRUCTURE

NGUYEN VAN GIAI and A. BOUYSSY
Division de Physique Théorique*, Institut de Physique Nucléaire,
F-91406 Orsay Cedex, France

Abstract

Some recent works related with relativistic models of nuclear structure are briefly reviewed. The Dirac-Hartree-Fock and Dirac-Brueckner-Hartree-Fock are recalled and illustrated by some examples. The problem of isoscalar current and magnetic moments of odd nuclei is discussed. The application of the relativistic model to the nuclear response function is examined.

1. INTRODUCTION

The traditional microscopic description of nuclear systems based on the picture of non-relativistic nucleons whose motion is governed by a Schrödinger equation and interacting via meson exchanges has by now reached a high level of sophistication. It has achieved good success sometimes at the expense of serious complications, but is has also met with some shortcomings, e.g. the saturation point of nuclear matter or the spin-orbit splittings in nuclei, to name the most obvious ones. Also, its extrapolation to systems far from normal density is probably unreliable. On the other hand, a relativistic field theory of nuclei should be a very satisfactory starting point to understand the non-relativistic approach, but unfortunately a complete theory does not exist yet. There are, however, many efforts to incorporate the field-theoretic aspects of nucleons and mesons in the description of nuclei, and this leads to a picture where the motion of nucleons in a medium obeys a Dirac equation. This is generally called the relativistic approach to nuclear structure, and we shall discuss in this paper some of these attempts.

The common feature of the various works in this field is to assume a lagrangian for the system of interacting nucleons and mesons. This lagrangian is then treated in the mean field (Hartree) or the Hartree-Fock (HF) approximation. The main outcome is that the nucleon self-energy has very strong (several hundreds MeV) Lorentz scalar and vector components of opposite signs. Ref.[1] contains a recent review of the numerous studies done along these lines. These findings were comforted by the success of phenomenological analyses [2] of medium energy proton scattering and by Dirac impulse calculations [3], which indicate that the scalar and vector components of the optical potential are very similar to the corresponding self-energies obtained in the Hartree approximation.

Another line of approach consists in requiring that the starting lagrangian describes correctly the scattering properties of the nucleon-nucleon system, and this fixes all the masses and coupling constants. The many-body problem is then treated in the Dirac-Brueckner (DH)

---

*Laboratoire associé au C.N.R.S.

IPNO/TH 87-4

approximation. This approach was adopted in Refs.[4-6]. Ref.[7] contains a review of the work done by Shakin's group. The results of the different authors do not always agree, but the strong cancellation between large scalar and vector self-energies again emerges.

An apparent drawback of the relativistic approach was pointed out long ago : the calculated magnetic moments of odd nuclei deviate strongly from the Schmidt values, and hence from experiment [8]. This subject has received considerable attention recently, and a satisfactory explanation seems to appear, at least for the isoscalar magnetic moment : there are large core contributions due to the vector meson which compensate the enhancement caused by the scalar meson [9-11].

The relativistic approach has also been used to study the nuclear excitations, especially the nuclear response functions and Coulomb sum rules measured in inclusive (e,e') experiments [12,13]. Recently, Suzuki has examined the predictions of the model concerning the energies of giant resonances [14]. All these studies can be considered as preliminary, and this domain of application of the relativistic approach is still in its infancy.

In section II, we present a Dirac-Hartree-Fock study of nuclear matter and finite nuclei. The Dirac-Brueckner approach to nuclear matter is discussed in section III. The problem of magnetic moments is examined in section IV. In section V, we briefly review the application of the relativistic approach to the nuclear response functions.

II. DIRAC-HARTREE-FOCK

The point of view adopted in the Dirac-Hartree-Fock (DHF) approach can be stated in the following way. One starts from a model lagrangian describing interacting nucleons and mesons, and this lagrangian is treated in the Hartree or Hartree-Fock approximation. In principle, all masses and coupling constants can be considered as parameters to be determined by adjusting the saturation properties of nuclear systems. In practice, there is no need for so many parameters and the masses and coupling constants of the nucleon and the best known mesons are fixed at their experimental values.

II.1 - Model lagrangian and approximate hamiltonian

We start with an effective lagrangian density $\mathcal{L}$ for a system of nucleons and four types of mesons : σ ($J^\pi = 0^+, T=0$), ω ($1^-, 0$), $\vec{\pi}$ ($0^-, 1$) and $\vec{\rho}$ ($1^-, 1$). For the pion, we choose the pseudo-vector (PV) coupling because it leads to a weaker coupling to negative energy states and hence gives more reasonable results. Thus, we work with a non-renormalizable effective lagrangian but it has the advantage of incorporating the physically important π- and ρ-mesons and can be compared to the N-N interaction used in the Dirac-Brueckner approach (see next section). With the Bjorken-Drell conventions [15], the lagrangian takes the form :

$$\mathcal{L} = \bar{\psi}\left(i\partial\!\!\!/ - M\right)\psi + \frac{1}{2}\left(\partial_\mu\sigma\partial^\mu\sigma - m_\sigma^2\sigma^2\right) + \frac{1}{2}m_\omega^2\omega_\mu\omega^\mu - \frac{1}{4}F_{\mu\nu}F^{\mu\nu}$$
$$+ \frac{1}{2}m_\rho^2\vec{\rho}_\mu\cdot\vec{\rho}^\mu - \frac{1}{4}\vec{G}_{\mu\nu}\cdot\vec{G}_{\mu\nu} + \frac{1}{2}\left(\partial_\mu\vec{\pi}\cdot\partial^\mu\vec{\pi} - m_\pi^2\vec{\pi}^2\right) + \mathcal{L}_I \quad , \qquad (II.1)$$

where $F_{\mu\nu}$ and $\vec{G}_{\mu\nu}$ are related to the ω- and ρ-fields by

$$F_{\mu\nu} = \partial_\nu\omega_\mu - \partial_\mu\omega_\nu \quad , \quad \vec{G}_{\mu\nu} = \partial_\nu\vec{\rho}_\mu - \partial_\mu\vec{\rho}_\nu \quad , \qquad (II.2)$$

whereas the interaction lagrangian $\mathcal{L}_I$ is :

$$\mathcal{L}_I = -g_\sigma \bar{\Psi}\sigma\Psi - g_\omega \bar{\Psi}\gamma_\mu \omega^\mu \Psi + \frac{f_\omega}{2M}\bar{\Psi}\sigma_{\mu\nu}\partial^\nu\omega^\mu\Psi$$
$$- g_\pi \bar{\Psi}\gamma_5 \vec{\tau}\vec{\pi}\Psi + \frac{f_\pi}{2M}\bar{\Psi}\sigma_{\mu\nu}\partial^\nu\vec{\pi}\vec{\tau}\Psi - \frac{f_\pi}{m_\pi}\bar{\Psi}\gamma_5\gamma^\mu\partial_\mu\vec{\pi}\vec{\tau}\Psi \quad (II.3)$$

We have not written explicitly the photon terms, but their inclusion presents no difficulty. In the following, the f_ω term is neglected because the physical value of the ratio $f_\omega / g_\omega = -0.12$ is small.

From this lagrangian density, it is convenient to derive a hamiltonian acting only in nucleon space, and this can be done by a standard procedure [16,17]. The first step is to demand that the action integral of $\mathcal{L}$ be stationary with respect to all variations of the fields. This leads to a set of coupled equations for the baryon and meson fields which enables one to express formally $\mathcal{L}$ in terms of $\Psi, \bar{\Psi}$ and the meson propagators. Then, by the Legendre transformation which relates the hamiltonian H to the lagrangian [1], one obtains H in the general form :

$$H = \int_{t_1=0} \bar{\Psi}(\underline{x}_1)(-i\vec{\gamma}.\vec{\nabla} + M)\Psi(\underline{x}_1)\, d^3x_1$$
$$+ \frac{i}{2}\sum_{\substack{i=\sigma,\omega,\\ \rho,\pi}} \int_{t_1=0} \bar{\Psi}(\underline{x}_1)\bar{\Psi}(\underline{x}_2)\, D_i(\underline{x}_1,\underline{x}_2)\,\Psi(\underline{x}_2)\Psi(\underline{x}_1)\, d^3x_1 d^4x_2 \quad , \quad (II.4)$$

where $\underline{x} = (t,\vec{x})$, and D_i depend on the meson propagators and the meson-nucleon couplings.

The hamiltonian (II.4) is exact but we don't know its solutions. The usual method for treating it in the DHF approximation is to use the Dyson equation for the baryon propagator [1]. It is possible to arrive at the same result by defining an approximate hamiltonian in the following way. We look for approximate field operators $\Psi_0(\underline{x})$ satisfying a Dirac equation with a self-energy Σ to be determined self-consistently :

$$(-i\vec{\partial} + M + \Sigma)\Psi_\alpha(\underline{x}) = 0 \quad . \quad (II.5)$$

By replacing the exact $\Psi(\underline{x})$ in eq.(II.4) by the approximate $\Psi_0(\underline{x})$ we obtain an effective hamiltonian H_0. The expectation value of H_0 in the HF state (Slater determinant) gives an energy E_0. When we minimize E_0 with respect to Σ, we shall obtain equations for Σ which will be seen to be identical to those obtained by the Dyson equation method.

The approximate nucleon fields $\Psi_0(\underline{x})$ can be expanded on the set of creation and annihilation operators defined by the stationary solutions of eq.(II.5), still to be determined :

$$\Psi_0(\underline{x}) = \sum_\alpha \left[f_\alpha(\vec{x})\, e^{-iE_\alpha t}\, b_\alpha + g_\alpha(\vec{x})\, e^{iE'_\alpha t}\, d^\dagger_\alpha \right] \quad , \quad (II.6)$$

where f_α and g_α are Dirac spinors. b_α and $b^\dagger_\alpha$ represent annihilation and creation operators for nucleons in a state α whereas d_α and $d^\dagger_\alpha$ are the corresponding operators for antinucleons.

The DHF approximation merely means self-consistent inclusion of exchange corrections to the mean field (Hartree) approach and therefore to keep the same level of approximation the d^+ terms are omitted in (II.6). Note that the neglected terms correspond to self-consistent negative energy states.

One more simplifying assumption is made by neglecting the time dependence of the meson fields, i.e. neglecting the time component of the four-momentum carried by the mesons. This has no consequence on the direct (Hartree) terms whereas for the Fock terms it amounts to neglect retardation effects, which should be acceptable since the energy transfers are generally small compared to meson masses. Then, H_o is simply the sum of a kinetic term and a two-body interaction term containing contributions of the various exchanged mesons. For instance, in momentum representation H_o takes the form :

$$H_o = \sum_{p_1,\alpha_1} \bar{u}(p_1,\alpha_1)\left[\vec{\gamma}.\vec{p} + M\right] u(p_1,\alpha_2)\, b^+_{p_1,\alpha_1} b_{p_1,\alpha_2}$$

$$+ \sum_\lambda \sum_{p_1,\alpha_1,\alpha_1'} \sum_q (i\sigma_\lambda)_\lambda \bar{u}(p_1+q,\alpha_1')\, \bar{u}(p_2-q,\alpha_2')\, \Gamma_\lambda(1,2)$$

$$\times \frac{1}{m_\lambda^2+\vec{q}^2}\, u(p_2,\alpha_2)\, u(p_1,\alpha_1)\, b^+_{p_1+q,\alpha_1'}\, b^+_{p_2-q,\alpha_2'}\, b_{p_2,\alpha_2}\, b_{p_1,\alpha_1} \quad . \tag{II.7}$$

Here, $u(p,\alpha)$ is a positive energy spinor with four-momentum $\underline{p} = (p_o,\vec{p})$ and spin-isospin quantum numbers α. The isospin factor is 1 for isoscalar mesons and $\vec{\tau}_1.\vec{\tau}_2$ for isovector ones. The operators Γ_λ are listed in Table 1.

II.2 - Nuclear matter

In an infinite medium, the general form of the self-energy Σ satisfying time-reversal and rotational invariance is :

$$\Sigma(\underline{p}) = \Sigma_s(\underline{p}) + \gamma_o \Sigma_o(\underline{p}) + \vec{\gamma}.\hat{p}\, \Sigma_v(\underline{p}) \quad , \tag{II.8}$$

where $\hat{p}$ is the unit vector along $\vec{p}$, and $\underline{p} = (E(\underline{p}),\vec{p})$ with $E(\underline{p})$ being the eigenvalue of the stationary solution of (II.5). The advantage of an infinite medium, similarly to the non-relativistic case, is that the form of the solutions is obvious. Indeed, if we introduce the following starred quantities :

$$\begin{aligned} \vec{p}^{\,*}(\underline{p}) &= \vec{p} + \hat{p}\, \Sigma_v(\underline{p}) \\ M^*(\underline{p}) &= M + \Sigma_s(\underline{p}) \\ E^*(\underline{p}) &= E(\underline{p}) - \Sigma_o(\underline{p}) \end{aligned} \tag{II.9}$$

it can be seen that eq.(II.5) is similar to a free-particle Dirac equation, and we can write down immediately the stationary solutions of (II.5) corresponding to positive energies :

$$u(\vec{p},\lambda) = \left(\frac{E^* + M^*}{2E^*}\right)^{1/2} \begin{pmatrix} 1 \\ \frac{\vec{\sigma}\cdot\vec{p}^*}{E^*+M^*} \end{pmatrix} \chi_\lambda \qquad \text{(II.10)}$$

Here, χ_s is a 2-component spinor and we have omitted for simplicity isospin variables. The adopted normalization is $u^+u = 1$. Note that the effective mass, momentum and energy (II.9) ae related by :

$$E^{*2} = \vec{p}^{*2} + M^{*2} \qquad \text{(II.11)}$$

It will be useful to introduce the quantities :

$$\hat{P} = \frac{p^*}{E^*} \quad , \quad \hat{M} = \frac{M^*}{E^*} \qquad \text{(II.12)}$$

In symmetric (N=Z) nuclear matter, the Hf trial state is :

$$|\phi_o\rangle = \left(\prod_{\vec{p},\lambda} b^+_{\vec{p},\lambda}\right)|0\rangle \qquad \text{(II.13)}$$

where $|0\rangle$ is the physical vacuum. We calculate the energy per particle E/A by taking the expectation value of H_0 in $|\phi_0\rangle$ over a given volume Ω and dividing by the numberof particles in Ω . The result is (with the nucleon mass subtracted) :

$$\frac{E}{A} = \frac{1}{\rho_B}\left[T + V_D + V_E\right] - M \qquad \text{(II.14)}$$

where $\rho_B = (2/3\pi^2)p_F^3$ is the baryonic density with p_F being the fermi momentum, and T, V_D, V_E are respectively the kinetic, Hartree (direct) and Fock (exchange) contributions. Their expressions are :

$$\begin{aligned} T &= \frac{2}{\pi^2}\int_0^{p_F} p^2 dp \left[p\hat{P} + M\hat{M}\right] \\ V_D &= -\frac{1}{2}\left(\frac{g_\sigma}{m_\sigma}\right)^2 \rho_S^2 + \frac{1}{2}\left(\frac{g_\omega}{m_\omega}\right)^2 \rho_B^2 \\ V_E &= \frac{1}{(2\pi)^3}\int_0^{p_F} p\,dp\, p'dp' \left\{\sum_\lambda \left[A_\lambda(p,p') + \hat{M}(p)\hat{M}(p')B_\lambda(p,p') \right.\right. \\ &\qquad \left.\left. + \hat{P}(p)\hat{P}(p')C_\lambda(p,p')\right] + \hat{P}(p)\hat{M}(p')D(p,p')\right\} \end{aligned} \qquad \text{(II.15)}$$

where

$$\rho_S = \frac{2}{\pi^2}\int_0^{p_F} p^2 dp\ \hat{M}(p) \qquad \text{(II.16)}$$

is the scalar density. Only isoscalar mesons contribute to Hartree terms whereas all mesons are present in Fock terms. The functions A_λ, B_λ, C_λ and D depend on coupling constants

and masses. Their expressions are lengthy and can be found in ref.[17].

The saturation curve is obtained by demanding that for each value of p_F, E/A must be minimum with respect to variations of $\vec{p}^*$ and M^* such that (II.11) be fulfilled. The saturation point corresponds to the value of p_F for which E/A is lowest. The self-energy Σ can be obtained by differentiating $(V_D - V_E)$ with respect to $u(\vec{p},s)$.

The following masses and coupling constants were kept fixed at their physical values: M = 938.9 MeV, m_ω = 783 MeV, m_ρ = 770 MeV, m_π = 138 MeV, $f_\pi^2/4\pi$ = 0.08 and $g_\rho^2/4\pi$ = 0.55. Furthermore, the ratio f_ρ/g_ρ is taken to be 3.7 according to the vector dominance model. Larger values of this ratio are sometimes favored, but we expect that working here with a smaller value of f_ρ somehow compensates for the lack of short range correlations in the HF approximation. For the same reason, the zero-range repulsive contributions from the PV π-coupling and T ρ-coupling were removed from H_D [17]. There remain 3 parameters to adjust the saturation point E/A = - 15.75 MeV at p_F = 1.30 fm^{-1}. Although nuclear matter is mostly sensitive to g_σ/m_σ and leaves m_σ largely undetermined, the study of finite nuclei (see next subsection) fixes the optimum value of m_σ = 440 MeV. Finally, the two remaining effective coupling constants are $g_\omega^2/4\pi$ = 4.16 and $g_{\omega\rho}^2/4\pi$ = 11.16. Table 2 gives the separate contributions of the mesons to E/A at the saturation point. Table 3 shows the bulk properties of nuclear matter calculated in the present DHF model. We notice the relatively small effective mass and the large *compression modulus which* are characteristic features of Dirac-Hartree and DHF approaches. In Fig.1 is shown the saturation curve calculated in DHF. It is very close to that obtained in a (σ,ω)-Hartree calculation but with strongly renormalized coupling constants to compensate for the lack of exchange contributions and isovector mesons. Fig.2 shows the momentum dependence of the different components of the self-energy. The single particle spectrum is given in Fig.3.

The net value of E/A results from strong cancellations between large contributions of the various mesons (see Table 2). The saturation mechanism is best illustrated by the simple (σ,ω)-Hartree model. In this case eqs.(II.14-15) become :

$$\frac{E}{A} = \frac{2}{\pi^2}\frac{1}{\rho_B}\int_0^{p_F} p^2\,dp\left[p\hat{P} + M\hat{M}\right] - \frac{1}{2}\left(\frac{g_\sigma}{m_\sigma}\right)^2\frac{\rho_S^2}{\rho_B} + \frac{1}{2}\left(\frac{g_\omega}{m_\omega}\right)^2\rho_B - M \quad . \qquad (II.17)$$

At large p_F, ρ_S goes to a finite value while ρ_B increases like p_F^3, so that the saturation curve is dominated by the repulsive ω-exchange. At low p_F, it is the kinetic term which takes over. It is the *delicate balance* between the σ-attraction and ω-repulsion which gives the minimum in the saturation curve. This balance depends crucially on the relativistic treatment, and the same lagrangian treated non-relativistically would not lead to saturation.

II.3 - Finite nuclei

Having determined the parameters of the effective lagrangian by the above study of infinite matter, we now examine how the same lagrangian can describe finite nuclei in *the DHF approximation*. Unlike the case of infinite medium, the analytical form of the self-consistent spinor cannot be guessed in advance and therefore it takes more numerical effort to calculate them.

For a spherical, closed-subshell nucleus containing A nucleons, a single particle baryon state will be specified by the set of quantum numbers $\alpha \equiv (\varepsilon_\alpha, q_\alpha, n_\alpha, \ell_\alpha, m_\alpha) \equiv (a, m_a)$ where $q_a = -1(+1)$ for a neutron(proton). The baryon spinor in coordinate representation is:

the same way spin-orbit doublets. Table 4 shows a remarkable agreement of calculated and experimental values of Δ_{LS}. The role of the π - and ρ -meson is very important for predicting correctly Δ_{LS}. The ability to describe correctly spin-orbit splittings, together with the special saturation mechanism, are two distinct features of the DHF approach which have no counterpart in the non-relativistic HF models.

III. DIRAC-BRUECKNER

In this approach, the starting point is to build a covariant model of the N-N interaction which can describe quantitatively the low and intermediate energy properties of the N-N system. This model is the one-boson exchange (OBE) which turns out to be quite successful in reproducing the N-N data. The next step is to use this OBE potential to solve the double self-consistent Brueckner problem in infinite matter in a covariant framework, and this is called the Dirac-Brueckner (DB) approach. It is well known that the non-relativistic Brueckner calculations of nuclear matter with realistic N-N interactions miss the phenomenological saturation point : all results lie on the so-called Coester line, and one has to invoke additional density-dependent effects brought in by three-body forces to improve the calculated saturation point. In the relativistic approach, the genuine density dependence due to the Brueckner method is sufficient to bring the saturation density to a reasonable value. Furthermore, a natural inclusion of some three-body effects can be made if one allows for Δ -propagation in intermediate states. Since the DB approach seems to describe adequately nuclear matter at normal density, it can be hoped that its extension to higher densities is sound and can provide a better equation of state than the non-relativistic approach. Here, we shall recall some of the results of ref.[6] where the double self-consistency calculations and the study of the role of the Δ were carefully carried out.

III.1 - The two-body problem

The two-particle interaction is represented by the covariant T-matrix $T^{(4)}$ which satisfies the Bethe-Salpeter equation :

$$T^{(4)} = K + K G^{(0)} G^{(0)} T^{(4)} \quad , \tag{III.1}$$

where K is the lowest order two-particle diagram and $G^{(0)}$ is the relativistic free particle propagator :

$$G^{(0)}(\not p) = (\not p - M + i\epsilon)^{-1} \quad . \tag{III.2}$$

It is customary to reduce (III.1) to a three-dimensional quasi-potential equation easier to solve :

$$\langle \vec p_1' \vec p_2' | T^{(3)}(\Lambda) | \vec p_1 \vec p_2 \rangle = \langle \vec p_1' \vec p_2' | V(\Lambda) | \vec p_1 \vec p_2 \rangle + \frac{1}{(2\pi)^3} \int d^3k$$

$$\times \langle \vec p_1' \vec p_2' | V(\Lambda) | \vec p_1^{\,*} \vec p_2^{\,*} \rangle\, g(\vec k, \Lambda) \langle \vec p_1^{\,*} \vec p_2^{\,*} | T^{(3)}(\Lambda) | \vec p_1 \vec p_2 \rangle \quad , \tag{III.3}$$

where $\Lambda = (\not p_1 + \not p_2)^2$, $\vec p_1^{\,*} = \frac{1}{2}(\vec p_1 + \vec p_2) + \vec k$, $\vec p_2^{\,*} = \frac{1}{2}(\vec p_1 + \vec p_2) - \vec k$.

$$\psi_\alpha(\vec{r}) = \frac{1}{r}\begin{pmatrix} iG_a(r) \\ F_a(r)\,\vec{\sigma}\cdot\hat{r} \end{pmatrix} \mathcal{Y}_a(\hat{r})\,\chi_{s_a} \quad , \tag{II.18}$$

where

$$\mathcal{Y}_a(\hat{r}) = \sum_{m_a m_s} (l_a\ \tfrac{1}{2}\ m_a\ m_s | j_a\ m_a)\, Y_{l_a}^{m_a}(\hat{r})\,\chi_{s_a} \quad , \tag{II.19}$$

and the spinors are normalized as :

$$\int d^3r\ \psi_\alpha^\dagger(\vec{r})\,\psi_\alpha(\vec{r}) = \int_0^\infty dr\,\left[G_a^2(r) + F_a^2(r)\right] = 1 \quad . \tag{II.20}$$

The DHF ground state is :

$$|\phi_0\rangle = \left(\prod_{\alpha(\text{occ.})} b_\alpha^\dagger\right)|0\rangle \quad . \tag{II.21}$$

The DHF equations for the unknown functions G_a, F_a and energies E_a are obtained by the variational condition :

$$\delta\left[E - \sum_{\alpha(\text{occ.})} E_\alpha \int \psi_\alpha^\dagger(\vec{r})\,\psi_\alpha(\vec{r})\,d^3r\right] = 0 \quad , \tag{II.22}$$

where $E \equiv \langle\phi_0|H_0|\phi_0\rangle - AM$ is the energy of the nucleus, and the E_a are Lagrange multipliers. The variations in (II.22) are with respect to the radial parts G_a and F_a of the spinor (II.18). After a lengthy calculation, the DHF equations are obtained in the form of coupled, inhomogeneous differential equations :

$$\frac{d}{dr}\begin{bmatrix} G_a(r) \\ F_a(r) \end{bmatrix} = \begin{bmatrix} -\frac{\kappa_a}{r} - \Sigma^\tau(r) & M + E_a + \Sigma^s(r) - \Sigma^o(r) \\ M - E_a + \Sigma^s(r) + \Sigma^o(r) & \frac{\kappa_a}{r} + \Sigma^\tau(r) \end{bmatrix}\begin{bmatrix} G_a(r) \\ F_a(r) \end{bmatrix} + \begin{bmatrix} -\chi_a(r) \\ Y_a(r) \end{bmatrix} , \tag{II.23}$$

Here, the local potentials Σ are direct contributions to the self-energy and their state dependence is only through the nucleon charge. The inhomogeneous terms χ and Y come from exchange contributions and they have a complicated state dependence. The quantity κ_a is $(2j_a+1)(l_a-j_a)$. The detailed expressions of the Σ, χ and Y can be found in ref.[17]. Eqs.(II.23) are then solved iteratively until convergence is reached.

Representative results of the DHF approach including the four mesons ($\sigma, \omega, \pi, \rho$) are shown in Table 4 and Fig.4. On the whole, results are better when going from a Hartree description with only σ and ω to a full DHF with both isoscalar and isovector mesons. Since center-of-mass effects have not been considered here, we have listed in Table 4 center-of-mass corrections taken from a non-relativistic HF calculation as an indicative estimate. One can see that about 1.5 MeV of binding energy per particle are missing for all nuclei. Correlation effects which are beyond the present approach could possibly increase the calculated binding energies. As we have mentioned in the previous subsection, the freedom on m_σ was used to adjust the size of the nuclei. With m_σ = 440 MeV, all proton radii come out very satisfactorily, and the charge densities shown in Fig.4 have a level of agreement with experiment quite comparable to that of non-relativistic HF calculations. Although the single particle spectra are different from the experimental ones (and there are good reasons for that!), a direct comparison between HF and measured spin-orbit splittings is probably justified since effects beyond HF which modify single particle energies should alter in

the same way spin-orbit doublets. Table 4 shows a remarkable agreement of calculated and experimental values of Δ_{LS}. The role of the π - and ρ -meson is very important for predicting correctly Δ_{LS}. The ability to describe correctly spin-orbit splittings, together with the special saturation mechanism, are two distinct features of the DHF approach which have no counterpart in the non-relativistic HF models.

III. DIRAC-BRUECKNER

In this approach, the starting point is to build a covariant model of the N-N interaction which can describe quantitatively the low and intermediate energy properties of the N-N system. This model is the ome-boson exchange (OBE) which turns out to be quite successful in reproducing the N-N data. The next step is to use this OBE potential to solve the double self-consistent Brueckner problem in infinite matter in a covariant framework, and this is called the Dirac-Brueckner (DB) approach. It is well known that the non-relativistic Brueckner calculations of nuclear matter with realistic N-N interactions miss the phenomenological saturation point : all results lie on the so-called Coester line, and one has to invoke additional density-dependent effects brought in by three-body forces to improve the calculated saturation point. In the relativistic approach, the genuine density dependence due to the Brueckner method is sufficient to bring the saturation density to a reasonable value. Furthermore, a natural inclusion of some three-body effects can be made if one allows for Δ -propagation in intermediate states. Since the DB approach seems to describe adequately nuclear matter at normal density, it can be hoped that its extension to higher densities is sound and can provide a better equation of state than the non-relativistic approach. Here, we shall recall some of the results of ref.[6] where the double self-consistency calculations and the study of the role of the Δ were carefully carried out.

III.1 - The two-body problem

The two-particle interaction is represented by the covariant T-matrix $T^{(4)}$ which satisfies the Bethe-Salpeter equation :

$$T^{(4)} = K + K G^{(0)} G^{(0)} T^{(4)} \quad , \tag{III.1}$$

where K is the lowest order two-particle diagram and $G^{(0)}$ is the relativistic free particle propagator :

$$G^{(0)}(\not p) = (\not p - M + i\varepsilon)^{-1} \quad . \tag{III.2}$$

It is customary to reduce (III.1) to a three-dimensional quasi-potential equation easier to solve :

$$\langle \vec{p}_1' \vec{p}_2' | T^{(3)}(\Lambda) | \vec{p}_1 \vec{p}_2 \rangle = \langle \vec{p}_1' \vec{p}_2' | V(\Lambda) | \vec{p}_1 \vec{p}_2 \rangle + \frac{1}{(2\pi)^3} \int d^3k$$

$$\times \langle \vec{p}_1' \vec{p}_2' | V(\Lambda) | \vec{p}_1'' \vec{p}_2'' \rangle \, Q(\vec{k}, \Lambda) \langle \vec{p}_1'' \vec{p}_2'' | T^{(3)}(\Lambda) | \vec{p}_1 \vec{p}_2 \rangle \quad , \tag{III.3}$$

where $\Lambda = (\not p_1 + \not p_2)^2$, $\vec{p}_1'' = \frac{1}{2}(\vec{p}_1 + \vec{p}_2) + \vec{k}$, $\vec{p}_2'' = \frac{1}{2}(\vec{p}_1 + \vec{p}_2) - \vec{k}$.

The quasi-potential V is a constrained form of K :

$$\langle \vec{p}_1', \vec{p}_2' | V(s) | \vec{p}_1, \vec{p}_2 \rangle = \langle \underline{p}_1' \underline{p}_2' | K | \underline{p}_1 \underline{p}_2 \rangle \quad , \qquad \text{(III.4)}$$

where the zero-components of $\underline{p}_1'$, $\underline{p}_2'$ are no longer independent but fixed by some choice of the off-shell position of particles 1 and 2. One possible choice is to put both particles symmetrically off-shell, i.e. $p_1^0 = p_2^0 = \frac{1}{2}\sqrt{s}$. This is the choice made in the Blankenbecler-Sugar [18] and Thompson [19] equations, and it corresponds to eq.(III.3) with :

$$g(\vec{k},s) = -i \int dk^0 \, G^{(0)}(\underline{k}) G^{(0)}(-\underline{k}) \quad . \qquad \text{(III.5)}$$

One further approximation for $g(\vec{k},s)$ is made by retaining only the positive-energy part of $G^{(0)}$ in (III.5). The resulting eq.(III.3) is the Thompson approximation [19].

In ref.[6] the above scheme has also been extended to include the $\Delta(3/2,3/2)$ degree of freedom, in which case eq.(III.3) becomes a set of coupled equations among the channels N-N, N-Δ and Δ-Δ. For the OBE interaction, six mesons were included : the four mesons of section II plus the η ($J^\pi = 0^+, T=0$) and the δ ($J^\pi = 0^+, T=1$). To account for the finite size of the baryons and to regularize the divergent character of the vector-meson exchanges, form factors are used at each vertex. They are taken of the monopole form $\Lambda_N^2/(\Lambda_N^2 - \vec{k}^2)$ for the N-N vertex, and of the dipole form $[\Lambda_\Delta^2/(\Lambda_\Delta^2 - \vec{k}^2)]^2$ for the N-Δ and Δ-Δ vertices.

In order to describe the two-body data, the authors of ref.[6] kept the meson masses fixed, and also assigned to the coupling constants g_π and g_ρ their experimental values. The remaining coupling constants and the cut-off masses Λ_N and Λ_Δ were then used as parameters to adjust calculated quantities to measured values. In Table 5 are shown the meson masses and coupling constants which give a good overall description of scattering cross-sections and polarizations as well as the scattering lengths and deuteron binding energy. For both parameter sets (B) and (C) (without and with Δ degree of freedom, respectively) one has $\Lambda_N^2 = 1.3$ GeV^2. In addition, $\Lambda_\Delta^2 = 0.63$ GeV^2 for set (C). In Figs. 5 and 6 are shown sample results of p-p angular distributions and polarizations. The importance of the Δ increases with increasing energy, especially if one looks at the polarizations. The general conclusion of this study is that, with a relatively small number of parameter the OBE model describes very satisfactorily a large body of data concerning the N-N system.

III.2 - Nuclear matter

A nucleon inside nuclear medium can be viewed as a particle dressed by its interactions with other particles. The dressed propagator $G(\underline{p})$ is given by the Dyson equation :

$$G(\underline{p}) = G^{(0)}(\underline{p}) + G^{(0)}(\underline{p}) \Sigma(\underline{p}) G(\underline{p}) \quad , \qquad \text{(III.6)}$$

where $G^{(0)}$ and Σ were introduced in (III.2) and (II.5). The self-energy Σ is given by the sum over vacuum-irreducible Feynman-type diagrams :

$$\Sigma(\underline{p}) = -i \int [dn] [G\Gamma] - G\Gamma]$$

$$= \sum_{\underline{p}' \text{(occ.)}} \left[\langle \underline{p}\,\underline{p}' | \Gamma | \underline{p}\,\underline{p}' \rangle - \langle \underline{p}\,\underline{p}' | \Gamma | \underline{p}'\,\underline{p} \rangle \right] \quad , \qquad \text{(III.7)}$$

where the states appearing in (III.7) are self-consistent, dressed states. The effective interaction in the medium Γ satisfies a medium-modified Bethe-Salpeter equation (or more precisely, a Thompson equation) analogous to (III.3), the main difference being the appearance of a Pauli exclusion operator Q in the intermediate states :

$$\langle \vec{p}_1' \vec{p}_2' | \Gamma(\omega) | \vec{p}_1 \vec{p}_2 \rangle = \langle \vec{p}_1' \vec{p}_2' | V(\omega) | \vec{p}_1 \vec{p}_2 \rangle + \frac{1}{(2\pi)^3} \int d^3k \tag{III.8}$$

$$\times \langle \vec{p}_1' \vec{p}_2' | V(\omega) | \vec{p}_1'' \vec{p}_2'' \rangle \, g(\vec{k}, \omega) Q(\vec{k}, \vec{p}_1 - \vec{p}_2, \omega) \langle \vec{p}_1'' \vec{p}_2'' | \Gamma(\omega) | \vec{p}_1 \vec{p}_2 \rangle \quad ,$$

with the notations of eqs.(III.3-III.5). Again, all the states in (III.8) are dressed ones, i.e. they are given explicitly by (II.10) with the starred quantities defined in (II.9). The operator Q is complicated, and it is in its handling that the various authors differ. It is usually replaced by its angle average. Furthermore, the $\vec{p}_1 - \vec{p}_2$ dependence was neglected in refs.[4,5], whereas this approximation was not made in ref.[6]. Notice that in eq.(III.8), all states are calculated with a self-energy which varies continuously across the Fermi surface, so that the present approach corresponds to the so-called continuous choice in non-relativistic Brueckner theory. In ref.[6], the extension of the above scheme to include intermediate N-Δ states was also considered. In this case, (III.8) becomes a set of equations coupling the N-N and N-Δ channels, with the introduction of a dressed Δ propagator and a corresponding Δ self-energy.

With V(s) determined by the two-body problem, eqs.(II.9),(III.5) and (III.7) are solved iteratively until the double self-consistency is reached. Owing to the weak momentum dependence of $\Sigma(\underline{p})$ (it would be momentum independent in the absence of exchange terms) a further simplifying assumption is made in the actual calculation by taking Σ at $p = p_F$ in eqs.(II.9). In the same spirit as that adopted in the N-N problem, only positive energy contributions are retained in the propagators $G(\underline{p})$ and in the nuclear matter total energy. The energy per particle E/A can then be written in the same way as for the DHF approximation :

$$\frac{E}{A} = \frac{1}{\rho_B} \sum_{\substack{\vec{p} \\ p \le p_F}} \bar{u}(\vec{p}, s) \left[\vec{\gamma} \cdot \vec{p} + M + \frac{1}{2} \Sigma(\vec{p}) \right] u(\vec{p}, s) \; - \; M \quad , \tag{III.9}$$

where the dressed spinors $u(\vec{p},s)$ are those of eq.(II.10).

We now illustrate the DB approach with some typical results of ref.[6]. Fig.7 compares the saturation curve calculated with set (B) of Table 5 (without Δ) with other calculations, namely a "conventional" calculation without M^* effect where one sets $M^*=M$ in eq.(III.5) (curve B), and a non-relativistic variational calculation [20] where a phenomenological density-dependent interaction was included to fit the saturation point (curve FP). Fig.8 shows the saturation curves calculated without Δ (set (B) of Table 5) and with Δ (set (C)). In both cases, the saturation density is much closer to its empirical value than in a conventional Brueckner calculation. The compression modulus at the saturation point is found to be K = 250 MeV if the Δ is not included, and K = 150 MeV if the Δ is included. These are closer to the generally accepted value of 220 MeV than that obtained in the DHF calculation reported in sect.II. This difference might partly come from the lack of form factors in the DHF calculation leading to too much short range repulsion and a stiffer equation of state.

The saturation properties of the DB approach are very similar to those of the DHF. If we look at the parameters of set (B) of Table 3, they are rather close to those of the DHF calculation excepted that the η and δ mesons are absent in the latter. The largest difference seems to be in the value of $g_\sigma^2/4\pi$. However, the σ-masses were different in the two calculations and if we consider the ratios g_σ/m_σ they are again very close (remember that the contribution of the σ meson to nuclear matter binding energy is mostly sensitive to g_σ/m_σ). It seems therefore that the effective lagrangian of DHF differs from the lagrangian in the absence of nuclear medium only by small renormalizations of the meson masses and coupling constants.

It can be concluded that the DB approach is able to describe successfully the saturation properties of nuclear matter owing to a saturation mechanism different from the non-relativistic one (see sect.II). Its application to higher density regions can then give an equation of state which may be more reliable than that obtained in a non-relativistic approach. It would be interesting to study finite nuclei within this DB approach, perhaps through a local density approximation.

IV. MAGNETIC MOMENTS AND NUCLEAR CURRENTS

Much work has been devoted recently to the study of nuclear currents since there is here a possible source of discrepancy between non-relativistic and relativistic models. Waiting for clear and unambiguous tests of the different approaches, some attention has to be paid to the electromagnetic response of nuclei and to the magnetic moments of odd nuclei with an extra-particle or hole.

We start with an effective electromagnetic current operator written as

$$j^\mu(\underline{x}) = \bar\psi(\underline{x})\gamma^\mu Q\,\psi(\underline{x}) + \frac{1}{2M}\partial_\nu\left(\bar\psi(\underline{x})\,\lambda\,\sigma^{\mu\nu}\psi(\underline{x})\right) \quad , \tag{IV.1}$$

where Q is the charge

$$Q = \frac{1}{2}(1+\tau_3) \qquad (\tau_3 = +1 \text{ for a proton})$$

and λ the anomalous magnetic moment defined by

$$\lambda = \lambda_p\,\frac{1+\tau_3}{2} + \lambda_n\,\frac{1-\tau_3}{2} \tag{IV.2}$$
$$\equiv \frac{1}{2}\left(\kappa_S + \kappa_V\tau_3\right)$$

where

$$\lambda_p = 1.793 \qquad \kappa_S = -0.120$$
$$\text{or equivalently} \tag{IV.3}$$
$$\lambda_n = -1.913 \qquad \kappa_V = 3.706$$

From eq.(IV.1) the three-vector current operator in the Schrödinger picture can be written as

$$\vec j(\vec r) = \psi^\dagger(\vec r)\,Q\,\vec\alpha\,\psi(\vec r) + \frac{1}{2M}\vec\nabla\times\left(\psi^\dagger(\vec r)\,\lambda\,\beta\,\vec\Sigma\,\psi(\vec r)\right) \quad , \tag{IV.4}$$

where the separation is made into the convection part and the magnetization part. In eq.(IV.4) $\vec{\alpha}$ and β are the usual Dirac matrices and

$$\vec{\Sigma} = \begin{pmatrix} \vec{\sigma} & 0 \\ 0 & \vec{\sigma} \end{pmatrix} .$$

The magnetic moment operator is defined as usual by :

$$\vec{\mu} = \int (\vec{r} \times \vec{j}) \, d^3r \quad ,$$

a quantity which reduces, in the non-relativistic case, to :

$$\vec{\mu}_{NR} = Q(\vec{l} + \vec{\sigma}) + \frac{1}{2}\vec{\sigma}(\kappa_s + \kappa_v \tau_3) \quad , \qquad \text{(IV.5)}$$

where the first term is the Dirac moment $\vec{\mu}_D$, the second one being the anomalous Pauli contribution $\vec{\mu}_A$.

In the case of odd nuclei adjacent to closed shells, the expectation value of $\vec{\mu}$ gives the usual Schmidt values

$$\mu_S = Q(\ell+1) + \lambda \qquad \text{if } j = \ell + \tfrac{1}{2}$$
$$= \frac{2\ell-1}{2\ell+1}(Q\ell - \lambda) \qquad \text{if } j = \ell - \tfrac{1}{2} \qquad \text{(IV.6)}$$

It is actually more convenient to look at isovector and isoscalar magnetic moments since experimental values exhibit deviations from the Schmidt values which can be explained by different origins [21]. The isovector moments are highly model dependent and receive large contributions from meson (pion and rho) exchange currents, core polarization and isobar currents. Isoscalar moments, on the other hand, are much better understood and receive contributions from second-order core polarization induced through the tensor interaction. We shall therefore concentrate mainly our discussion on isoscalar quantities.

Table 6 compares the isoscalar Schmidt values with the experimental quantities for nuclei in the vicinity of A = 16 and 40. The agreement is better for (A-1) nuclei but it is certainly no perfect.

Relativistic corrections to the Schmidt values have been studied in the framework of the relativistic mean field model of Walecka and co-workers [1] restricted to σ and ω - meson exchanges. A first step towards a modeling of a A-1 system is simply to create a particle or hole on top of the occupied levels. One then assumes that the wave function of the core is not altered in the new system. Therefore, when calculating the expectation value of the magnetic moment operator, only matrix elements of the valence nucleon remain, since the core contribution vanishes.

Using the Hartree wave functions as determined previously (see sect.II) the magnetic moment results in the contribution of 2 terms [5] :

$$\mu = \mu_D^{(0)} + \mu_A^{(0)} \quad ,$$

$$\mu_D^{(0)} = \mp Q \frac{2j+1}{j+1} M \int r\, F(r)\, G(r)\, dr \quad , \tag{IV.7a}$$

$$\mu_A^{(0)} = \pm\lambda \left(\frac{j}{j+1}\right)^{1/2} \left\{ \left(\frac{j}{j+1}\right)^{\mp\frac{1}{2}} \int G^2(r)\, dr + \left(\frac{j}{j+1}\right)^{\pm\frac{1}{2}} \int F^2(r)\, dr \right\} \quad , \tag{IV.7b}$$

with the $\mp$ signs corresponding to $j = \ell \mp 1/2$ respectively. Because of the normalization of the wave function, $\int (G^2+F^2)dr = 1$, the anomalous part is rather insensitive to the degree of relativity. This is not the case for the Dirac part. Significant deviations from the Schmidt value are thus found [22], which can be traced back to the effective mass M^* of the valence nucleon. The effective mass M^* differs significantly from the free mass M ($M^*(r=0)/M \simeq 0.6$) due to the large scalar field corresponding to the σ meson. Results for the isocalar megnetic moments as determined from eqs.(IV.7) are given in Table 6.

Different possibilities to cure such a disturbing failure of relativistic models have been proposed [9,10]. The large discrepancy between Schmidt and relativistic values can be eliminated by realizing that the response of the nuclear core to the valence nucleon cannot be neglected when evaluating isoscalar currents in the relativistic model. In principle, one should therefore calculate the ground states of $A \pm 1$ nuclei in a fully self-consistent fashion, instead of using the single-particle plus core picture. Since this kind of calculation is not yet available, a first step in this direction is to study nuclear matter with one nucleon added to the filled Fermi sphere and then use a local density approximation (LDA) to study implications for finite nuclei.

It has been realized that a distinction has to be made between nuclear velocities and nuclear currents, since in an interacting many-body system gauge invariance has to be taken into account. In nuclear matter the velocity of a valence nucleon at the fermi surface is given by

$$\vec{v} = \frac{\vec{k}_F}{E_F^*} \quad , \tag{IV.8}$$

which corresponds to $\langle \bar{\Psi} \vec{\alpha} \Psi \rangle$, the fermi energy being $E_F^* = (k_F^2 + M^{*2})^{1/2}$. Gauge invariance demands that the external field also interacts with particles in the medium and not only with the valence particle [23] (see Fig.9). As a result, in the framework of a Fermi liquid theory, Matsui [24] has shown that the self-consistent baryon current is not obtained from eq.(IV.8) but rather from

$$\vec{j} = \frac{\vec{k}_F}{E_F^*} \left[1 + \frac{g_\omega^2}{m_\omega^2} \frac{\rho_B}{E_F^*} \right]^{-1} = \frac{\vec{k}_F}{E_F^*} \frac{E_F^*}{M^*} = \frac{\vec{k}_F}{M^*} \quad , \tag{IV.9}$$

where μ is the chemical potential, $\mu = E_F^* \cdot (g_\omega/m_\omega)^2 \rho_B$. The first factor, k_F/E_F^*, is the relativistically M/M^* enhanced vector current. The core response factor E_F^*/μ cancels the enhancement due to M^*, almost exactly, since the chemical potential differs from the free nuclear energy only from binding energy effects ($\mu \simeq M$). The baryon current is therefore close to its free value. This correction, often referred to as a backflow in Fermi liquid theory [25] comes from the space-part of the ω exchange [10].

A similar result has also been obtained by Kurasawa and Suzuki [9] who studied the response of the system in the framework of the relativistic RPA (RRPA) [26] in the $q^\mu \to 0$ limit where q^μ is the four-momentum transfer (more precisely, one must first let $\vec{q}$ tend to zero, then make $q^0 \to 0$). It has been shown [27] that the isoscalar vertex corrections obtained from Ward identities are just the transverse polarization insertion Π_T obtained in the RRPA. This correlation function is given in terms of the Hartree correlation function Π_T^H by :

$$\Pi_T = \frac{\Pi_T^H}{1 - (g_\omega/m_\omega)^2 \Pi_T^H} \quad , \tag{IV.10}$$

where the lowest order ring contribution, when evaluated in nuclear matter, is :

$$\Pi_T^H = - \rho_B \frac{E_F^*}{} \tag{IV.11}$$

After summing the rings to all orders, the total baryon current is given by :

$$\vec{j}_i = \frac{\vec{k}_i}{E_i^*} \left(1 + (g_\omega/m_\omega)^2 \Pi_T \right) \quad , \tag{IV.12}$$

which can be rewritten, using eqs.(IV.10-IV.11) as :

$$\vec{j}_i = \frac{\vec{k}_i}{E_i^*} \left(1 + (g_\omega/m_\omega)^2 \frac{\rho_B}{E_F^*} \right)^{-1} \quad . \tag{IV.13}$$

This leads to the same factor as in eq.(IV.9). The connection between the different approaches has been discussed in details in refs.[IV.25]. The baryon current in both cases can then be written as

$$\vec{j} = \frac{\vec{k}}{(\vec{k}^2 + M^{*2})^{1/2}} \frac{1}{1+x} \quad , \tag{IV.14}$$

where the M^* enhancement corresponds to the scalar field while backflow reduction depends on the vector field.

In order to use the LDA to study implications for finite nuclei, the matrix element of the valence nucleon can be modified by multiplying each term in the current operator by the appropriate correction factor, evaluated at the local density. It is only the isoscalar

part of the current which is corrected by the backflow since the vector meson is isoscalar. Moreover, in this model it is only the convection piece which is corrected, the anomalous term being unchanged. In the calculation of the expectation value of μ one should make the replacement

$$\frac{1}{2}(1+\tau_3) \longrightarrow \frac{1}{2}\left(\frac{1}{1+\alpha(r)}+\tau_3\right) \qquad (IV.15)$$

where $\alpha(r)$, according to eqs.(IV.13-IV.14) is :

$$\alpha(r) = \frac{\left(g_\omega/m_\omega\right)^2 \rho_B(r)}{\left[\left(\frac{3\pi^2}{2}\rho_B(r)\right)^{2/3} + M^{*2}(r)\right]^{1/2}} \qquad (IV.16)$$

As a consequence eq.(IV.7) has to be replaced by

$$\mu_D = \mp \frac{2j+1}{j+1} M \int \frac{1}{2}\left(\frac{1}{1+\alpha(r)}+\tau_3\right) r\, F G\, dr \quad . \qquad (IV.17)$$

The isovector part of the Dirac magnetic moment is still enhanced (inclusion of the ρ meson in the σ-ω model gives very small effects). Since in addition pion effects which are certainly important for isovector moments are not taken into account in this model, there are significant theoretical uncertainties associated to isovector moments.

Results for isoscalar moments, calculated as indicated here, are shown in Table [redacted]. As expected from the nuclear matter evaluation, the moments are essentially back to their Schmidt values when core contributions are taken into account. This means that magnetic moments are insensitive to large values of the scalar field. These large values are necessary for the correct saturation and to get the right order of magnitude for the spin-orbit splitting and they lead to an effctive mass as small as half the bare mass.

As an alternative, in order to avoid the use of LDA and encouraged by the similarity in nuclear matter between the backflow and the RRPA, one can study the RRPA correction to the magnetic moment calculated directly for a finite system.

The lowest order RRPA contribution, shown in Fig.1D , to the magnetic moment is given schematically by

$$\Delta\vec{\mu} = \sum_{Bb} \frac{\langle AB|v|bA\rangle}{E_B - E_b}\left[\langle B|\vec{\mu}|b\rangle + \langle b|\vec{\mu}|B\rangle\right] \quad , \qquad (IV.18)$$

where the summation is performed over particle (B)-hole (b) bubbles. In eq.(IV.15) the interaction v corresponds to σ and ω exchanges. When only direct matrix elements are taken into account the space part of the ω -exchange only remains. Consequently, the magnetic moments are now written as :

$$\mu_D = \mu_D^{(0)} + \Delta\mu_D$$
$$\mu_A = \mu_A^{(0)} + \Delta\mu_A \quad , \qquad (IV.19)$$

where $\mu_{D,A}^{(o)}$ are given by eqs.(IV.7). The corrective term $\Delta\mu_D$ (resp. $\Delta\mu_A$) is the same whatever the extra particle is, proton or neutron, when the Coulomb interaction is neglected. This means in particular that the first order RRPA contribution to the Dirac moment of an extra-neutron is different from zero : the Dirac moment of an extra-neutron comes entirely from the corrective term. One ends up with isoscalar moments in the form :

$$\mu_D^{IS} = \mu_D^{IS(o)} \ (1 + \alpha)$$
$$\mu_A^{IS} = \mu_A^{IS(o)} \ (1 + \beta) \qquad , \tag{IV.20}$$

where $\mu_D^{IS(o)}$ and $\mu_A^{IS(o)}$ are the quantities given in the second column of Table 6.

Calculations [29] for A =15 systems indicate α = - 0.17 (-0.007 for A= 17 systems) while β is almost zero, since in that case the correction corresponds to radial excitations only. These results are quite encouraging, but obviously the complete RRPA solution is called for in order to compare to the calculation of ref.[9].

Many problems still remain. Isovector moments are here also enhanced but there is a need for a complete RPA calculation , where π and ρ mesons are contributing, before any definite conclusion can be drawn. It has however been shown that, either working in nuclear matter and using the LDA or direcly in finite nuclei, RPA type corrections corresponding to the response of the core when an extra-particle is added, have the tendency to reduce the isoscalar magnetic moments and bring them back close to their Schmidt values. This property is not peculiar to a relativistic system since the same kind of result occurs in the case of a non-relativistic calculation when galilean invariance is restored [30].

V. EXCITED STATES

The relativistic approach is not restricted to ground state properties but can also be applied to the study of nuclear excitations. We shall discuss briefly here the problems of nuclear response functions and some preliminary work on giant resonances. The question of response functions is especially interesting because in (e,e') experiments, it is possible to measure separately longitudinal and transverse responses R_L and R_T by choosing appropriate kinematics [31]. In the quasi-elastic peak region and beyond, energy and momentum transfers are such that a relativistic treatment of nuclear structure might be more adequate than a non-relativistic one. Indeed, it is found that the relativistic effective mass M^* brings sizable modifications to the longitudinal response R_L while R_T is less affected [12].

5.1 - Response functions in nuclear matter

We start with the simplest situation, that of relativistic nuclear matter described by a Dirac-Hartree model as in sect.II. Assuming for the moment that nucleons are point-like particles, we begin with the Coulomb response $R_C(\vec{q},\omega)$ of the system to the charge-density operator :

$$\rho(\vec{x}) = \sum_{\alpha} \psi^{\dagger}(\vec{x},\alpha)\, Q\, \psi(\vec{x},\alpha) \qquad . \tag{5.1}$$

The Coulomb response for a four-momentum transfer $q = (\omega, \vec{q})$ is :

$$R_c(\vec{q},\omega) = \sum_{n\neq 0} |\langle n|\rho(\vec{q})|0\rangle|^2 \, \delta(\omega-\omega_n) \quad , \tag{V.2}$$

where $|n\rangle$ is an excited state with excitation energy ω_n, and $\rho(\vec{q})$ is the Fourier transform of $\rho(\vec{x})$. In the present model, $|n\rangle$ is just a particle-hole state. It is useful to separate two classes of states : i) states where the hole is in the Fermi sea, denoted by $|n_F\rangle$. ii) states where the hole is in the Dirac sea, denoty by $|n_D\rangle$. We shall denote by $\vec{k}$ the momentum of the hole and by $\vec{k}+\vec{q}$ that of the particle. Because of energy-momentum conservation, it can be seen that the energies ω_{n_F}, ω_{n_D} are such that :

$$\begin{aligned} \omega_{n_F} &= E^*_{\vec{k}+\vec{q}} - E^*_{\vec{k}} \quad \leqslant |\vec{q}| \\ \omega_{n_D} &= E^*_{\vec{k}+\vec{q}} + E^*_{\vec{k}} \quad > |\vec{q}| \end{aligned} \tag{V.3}$$

The Coulomb response R_c can also be separated into a sum of a Fermi and a Dirac contribution [32] :

$$R_c(\vec{q},\omega) = R_c^F(\vec{q},\omega) + R_c^D(\vec{q},\omega) \quad , \tag{V.4}$$

where

$$R_c^F(\vec{q},\omega) = \sum_{\vec{k}} n_{\vec{k}}(1-n_{\vec{k}+\vec{q}}) \, \frac{(E^*_{\vec{k}+\vec{q}}+E^*_{\vec{k}})^2 - \vec{q}^{\,2}}{2E^*_{\vec{k}+\vec{q}}E^*_{\vec{k}}} \, \delta(\omega - E^*_{\vec{k}+\vec{q}} + E^*_{\vec{k}}) \, , \tag{V.5}$$

$$R_c^D(\vec{q},\omega) = -\sum_{\vec{k}} (1-n_{\vec{k}+\vec{q}}) \, \frac{(E^*_{\vec{k}+\vec{q}}-E^*_{\vec{k}})^2 - \vec{q}^{\,2}}{2E^*_{\vec{k}+\vec{q}}E^*_{\vec{k}}} \, \delta(\omega - E^*_{\vec{k}+\vec{q}} - E^*_{\vec{k}}) \quad . \tag{V.6}$$

In eqs.(V.5-V.6) appear the occupation numbers $n_k = 1$ if $|\vec{k}| \leqslant k_F$, 0 if $|\vec{k}| > k_F$.

By integrating $R_c(\vec{q},\omega)$ over ω at fixed $\vec{q}$, one obtains the so-called Coulomb sum rule $S_c(\vec{q})$. This quantity seems interesting because in a non-relativistic description, its limit when $|\vec{q}|\to\infty$ is the proton number Z, and this limit is model independent. Apart from the question of using a non-relativistic description to study an asymptotic momentum behaviour, it must be noted that this appealing result is obtained only if one integrates R_c^{NR} up to infinity in ω for fixed $\vec{q}$. However, this integral cannot be measured because the kinematics of the (e,e') reaction always require $\omega \leqslant |\vec{q}|$. Our separation of R_c into R_c^F and R_c^D is then convenient because the two components take their values in non-overlapping regions of ω separated by $|\vec{q}|$ (see (V.3)). By integrating R_c^F in the space-like ($\omega \leqslant |\vec{q}|$) region we obtain the physical Coulomb sum rule :

$$S_c^F(\vec{q}) = Z - \sum_{\vec{k}} n_{\vec{k}} n_{\vec{k}+\vec{q}} \frac{(E^*_{\vec{k}+\vec{q}} + E^*_{\vec{k}})^2 - \vec{q}^2}{2E^*_{\vec{k}+\vec{q}} E^*_{\vec{k}}} + \sum_{\vec{k}} n_{\vec{k}} \frac{(E^*_{\vec{k}+\vec{q}} - E^*_{\vec{k}})^2 - \vec{q}^2}{2E^*_{\vec{k}+\vec{q}} E^*_{\vec{k}}} \quad , \tag{V.7}$$

The integral of R_c^D in the time-like ($\omega > |\vec{q}|$) region gives the rest of the sum rule :

$$S_c^D(\vec{q}) = - \sum_{\vec{k}} (1 - n_{\vec{k}+\vec{q}}) \frac{(E^*_{\vec{k}+\vec{q}} - E^*_{\vec{k}})^2 - \vec{q}^2}{2E^*_{\vec{k}+\vec{q}} E^*_{\vec{k}}} \quad . \tag{V.8}$$

These results were already obtained by Matsui [33] and differ from those obtained by Walecka [34]. The reasons for this difference are discussed in ref.[32].

In Fig.11 is shown the behaviour of $S_c^F(\vec{q})$ for two different values of M^*. It must be noted that for $|\vec{q}|$ going to infinity, $S_c^F(\vec{q})$ tends to $Z/2$ in contrast with the non-relativistic result. The quantity $S_c^D(\vec{q})$ is divergent because of the infinite Dirac sea contribution. One should define a renormalization procedure to render it finite. In any case, it is not observable in the (e,e') reaction.

In real life, nucleons are not point-like but have a finite extension. What can be measured is not $R_c^F(\vec{q},\omega)$ but the longitudinal response $R_L(\vec{q},\omega)$. To take care of the nucleon finite size, one must introduce form factors. We write the nuclear current in the conventional form :

$$J^\mu(q) = F_1(q^2)\,\delta^\mu + i\lambda \frac{F_2(q^2)}{2M} \sigma^{\mu\nu} q_\nu \quad , \tag{V.9}$$

where λ was introduced in (IV.3). The form factors F_1 and F_2 can be related to the Sachs charge and magnetic form factors $G_E(q^2)$ and $G_M(q^2)$ by [15] :

$$\begin{aligned} F_1 + \lambda \frac{q^2}{4M^2} F_2 &= G_E \\ F_1 + \lambda F_2 &= G_M \end{aligned} \quad . \tag{V.10}$$

There are various phenomenological parametrizations of the Sachs form factors, and the comparison of different calculations of R_L is sometimes obscured by the different choices of G_E and G_M [13,32]. The expression of $R_L(\vec{q},\omega)$ in nuclear matter is [35] :

$$R_L(\vec{q},\omega) = \sum_{\vec{k}} \frac{n_{\vec{k}}(1 - n_{\vec{k}+\vec{q}})}{E^*_{\vec{k}}(E^*_{\vec{k}} + \omega)} \delta(\omega - E^*_{\vec{k}+\vec{q}} + E^*_{\vec{k}})$$

$$\times \left[2(E^*_{\vec{k}} + \frac{\omega}{2})^2 (F_1^2 - \frac{q^2}{4M^2}\lambda^2 F_2^2) - \frac{\vec{q}^2}{2}(F_1 + \frac{M^*}{M}\lambda F_2)^2 \right] \quad , \tag{V.11}$$

where only Fermi sea holes contribute because of the condition $\omega \leq |\vec{q}|$. In eq.(V.11) one must sum over neutrons and protons.

In Fig.12 we show the results obtained in ref.[36]. The function $R_L(\vec{q},\omega)/Z$ calculated with a (σ,ω) Dirac-Hartree model is compared to that of a non-relativistic Fermi gas. The effect of the effective mass M^* is to lower appreciably the height of the quasi-elastic peak. In ref.[36] the longitudinal response was also calculated in the framework of RRPA, and the results are shown in Fig.12. One can see that the RPA correlations lower further the response as compared to the uncorrelated case.

V.2 - Nuclear response in finite nuclei

There are a few calculations of R_L and R_T in finite nuclei, based on the (σ,ω) Dirac-Hartree model or some equivalent model. In ref.[12], a Foldy-Wouthuysen expansion in p/M^* (instead of the usual p/M expansion) was used to study the mechanism by which R_L and R_T are affected by the relativistic effective mass M^*. In comparison with a standard calculation using Woods-Saxon potentials, two effects were found. The first one is a Perey effect, i.e. a scattering wave function calculated with an r-dependent effective mass (non-locality effect) is smaller in the nuclear interior than the one calculated in a local potential, although both wave functions are identical asymptotically. This first effect tends to lower both R_L and R_T. The second effect is a renormalization of the current leading to a decrease of the longitudinal component and an increase of the transverse one. The net result is that the relativistic R_L is appreciably lowered whereas R_T is less affected as compared to their non-relativistic counterparts. The numerical application was made using phenomenological potentials fitted to elastic proton-nucleus scattering and an adjustable effective mass $M^*(r)$. The results are illustrated by Fig.13 where the value $M^*(r=0)/M = 0.53$ was used. The fact that the calculated transverse response underestimates the data in the high-ω region is not of serious concern because this region is dominated by the Δ-production and exchange current effects which are beyond the model.

In ref.[13] the (σ,ω) Dirac-Hartree model was used to calculate the response functions in ^{12}C and ^{40}Ca. As an example we show in Fig.14 the results for ^{12}C at $|\vec{q}| = 400$ MeV/c. The influence of nucleon form factors was stressed. The solid curves were obtained with the following choice (with q^2 in GeV) :

$$G_E^{(p)} = \left[1 - q^2/0.71\right]^{-2}$$

$$F_1^{(p)} = G_E^{(p)}\left[1 - \frac{q^2}{4M^2}(1+\lambda_p)\right]/\left[1 - \frac{q^2}{4M^2}\right]$$

$$F_2^{(p)} = G_E^{(p)}/\left[1 - \frac{q^2}{4M^2}\right] \qquad (V.12)$$

$$F_1^{(n)} = 0\,, \quad F_2^{(n)} = G_E^{(p)}$$

The dashed curves were calculated with the choice adopted in ref.[12], namely :

$$F_1^{(p)} = F_2^{(p)} = F_2^{(n)} = G_E^{(p)}\,, \quad F_2^{(n)} = 0 \qquad (V.13)$$

The longitudinal response calculated with the more correct choice (4.12) still overestimates the data whereas the transverse one is too low. There remains to see if the RPA correlations, which lower R_L in infinite matter (see Fig.12) can help to improve the longitudinal case without deteriorating further the transverse response. For the latter, it is likely that isovector mesons can play an important role and that the too simple (σ,ω) model is not sufficient.

V.3 - Giant resonances

The microscopic description of giant resonances in a relativistic approach is in a quite early stage. With the DHF or DB calculations, one has a starting point based on firm ground. The next step is to develop an RPA scheme which must be self-consistent as it was done in the non-relativistic approach with density-dependent effective interactions. This self-consistency is lacking in the attempt made in ref.[37] where the mean field and p-h residual interaction were not treated on the same level of approximation.

In a recent work, Nishizaki et al. [14] have studied the energies of the giant monopole and quadrupole states in the (σ,ω) model, using a scaling method. Assuming infinite matter, the excitation energies can be expressed in terms of relativistic Landau parameters. The expressions thus obtained are very similar to the non-relativistic ones. However, the values of the Landau parameters are such that the quantitative predictions are not in as good agreement with experiment as those of non-relativistic theories, at least for the (σ,ω) model. This was already expected for the monopole mode if one recalls the large incompressibility values coming from DHF calculations. This might perhaps be cured if one works with form factors like in the DB calculations. Another possibility is to add scalar-meson self-interactions to the (σ,ω) lagrangian, i.e. to have σ^3 and σ^4 terms in the lagrangian (II.1) restricted to (σ,ω). This was done in ref.[36] where these new terms (and new adjustable parameters) helped to bring the incompressibility to more acceptable values.

Besides detailed RRPA calculations, more global methods can be thought of. In non-relativistic self-consistent RPA, there exists a theorem which enables one to calculate the inverse energy-weighted moment M_{-1} of RPA just by performing a constrained HF calculation. Following this line, we have recently compared the monopole polarizability obtained by a DHF calculation with a monopole constraint, with that calculated by a RRPA diagonalization [39]. The two methods are in excellent agreement, a result which indicates that a relativistic version of the M_{-1} theorem probably holds.

VI. CONCLUDING REMARKS

The relativistic approach has proved its ability to describe nuclear phenomena in systems at normal density. It incorporates in a natural way the meson degrees of freedom which are known to be very important. Even at low energies, a relativistic formalism is not some kind of burden that one can live without. For instance, it brings specific mechanisms which help to understand the saturation properties. Being successful in describing systems near their normal state, it is by construction a firm ground for extrapolating towards more extreme conditions of densities or temperatures. Much more work remains to be done to refine this tool and to extend its field of application.

REFERENCES

[1] B.D. Serot and J.D. Walecka, Adv. Nucl. Phys. 16 (1986) 1.

[2] see, e.g., B.C. Clark et al., Phys. Rev. C28 (1983) 1421.

[3] see, e.g., J.A. Tjon and S.J. Wallace, Phys. Rev. C32 (1985) 267.

[4] C.J. Horowitz and B.D. Serot, Nucl. Phys. A399 (1983) 529 ; Phys. Lett. 137B (1984) 287.

[5] R. Brockmann and R. Machleidt, Phys. Lett. 149B (1984) 293.

[6] B. ter Haar and R. Malfliet (1986), submitted to Phys. Reports.

[7] L.S. Celenza and C.M. Shakin, Relativistic Nuclear Physics, World Scientific ed. (1986).

[8] L.D. Miller, Ann. Phys. (N.Y.) 91 (1975) 40.

[9] H. Kurasawa and T. Suzuki, Phys. Lett. 165B (1986) 234.

[10] J.A. Mc Neil et al., Phys. Rev. C34 (1986) 745.

[11] R.J. Furnstahl and B.D. Serot, preprint IU/NTC 86-3.

[12] C. Do Dang and Nguyen Van Giai, Phys. Rev. C30 (1984) 731.

[13] S. Nishizaki, H. Kurasawa and T. Suzuki, Phys. Lett. 171B (1986) 1.

[14] S. Nishizaki, H. Kurasawa and T. Suzuki, preprint RIFP-663 (1986).

[15] J.D. Bjorken and S.D. Drell, Relativistic Quantum Mechanics, Mc Graw Hill ed. (1964).

[16] R. Brockmann, Phys. Rev. C18 (1978) 1510.

[17] A. Bouyssy et al., preprint IPNO/TH 86-27.

[18] R. Blankenbecler and R. Sugar, Phys. Rev. 142 (1966)1051.

[19] R.H. Thompson, Phys. Rev. D1 (1970) 110.

[20] B. Friedman and V.R. Pandharipande, Nucl. Phys. A361 (1981) 502.

[21] I.S. Towner and F.C. Khanna, Nucl. Phys. A399 (1983) 334.

[22] A. Bouyssy et al., Nucl. Phys. A415 (1984)497.

[23] P.C. Blunden, preprint MIT-CTP 1340 (1986).

[24] T. Matsui, Nucl. Phys. A370 (1981) 365.

[25] G.E. Brown et al., preprint (1986).

[26] S.A.Chin, Ann. Phys.(N.Y.) 108 (1977) 301.

[27] W. Bentz et al., Nucl. Phys. A436 (1985) 593.

[28] J.A. Mc Neil, 2nd Conference on Intersection between Particle and Nuclear Physics, Lake Louise, Canada (1986).

[29] A. Bouyssy and Nguyen Van Giai, to be published.

[30] B. Desplanques, Z. für Physik A326 (1987).

[31] P. Barreau et al., Nucl. Phys. A402 (1983) 515.

[32] C. Do Dang, M. L'Huillier, Nguyen Van Giai and J.W. Van Orden, preprint IPNO/TH 86-76.

[33] T. Matsui, Phys. Lett. 132B (1983) 260.

[34] J.D. Walecka, Nucl. Phys. A399 (1983) 367.

[35] C. Do Dang and Pham Van Thieu, Phys. Rev. C28 (1983) 1645.

[36] H. Kurasawa and T. Suzuki, Phys. Lett. 154B (1985) 16.

[37] R.J. Furnstahl, Phys. Lett. 152B (1985) 313.

[38] A. Bouyssy, S. Marcos and Pham Van Thieu, Nucl. Phys. A422 (1984) 541.

[39] A. Bouyssy, Nguyen Van Giai and S. Marcos, to be published.

[40] B. Frois, Proc. Int. Conf. Nucl. Phys., Florence, Italy, p.221 (1983).

λ	$\Gamma^{\tau}_{\lambda}(1,2)$
σ	$-g_{\sigma}^2$
ω	$g_{\omega}^2 \gamma_{\mu}(1)\,\gamma^{\mu}(2)$
π(PV)	$-(f_{\pi}/m_{\pi})^2 (\vec{q}\,\vec{\gamma}_5)_1\,(\vec{q}\,\vec{\gamma}_5)_2$
ρ(V)	$g_{\rho}^2 \vec{\gamma}_{\mu}(1)\,\vec{\gamma}^{\mu}(2)$
ρ(T)	$(f_{\rho}/2M)^2\, q_{\nu}\,\sigma^{\beta\nu}(1)\, q^{\kappa}\,\vec{\sigma}_{\mu\kappa}(2)$
ρ(VT)	$i(f_{\rho}\, g_{\rho}/2M)[\vec{\gamma}_{\mu}(2)\sigma^{\mu\nu}(1)q_{\nu} - \sigma^{\mu\nu}(2)q_{\nu}\,\vec{\gamma}_{\mu}(1)]$

Table 1 - The operators $\Gamma^{\tau}_{\lambda}(1,2)$ of eq.(II.7). V : vector, T : tensor, VT : vector-tensor.

Kinetic	Direct		Exchange			
	σ	ω	σ	ω	π	ρ
9.2	-135.	131.	26.	-22.	-6.6	-19.

Table 2 - Kinetic and separate meson contributions (in MeV) to E/A in DHF.

K(MeV)	a_4(MeV)	M^*/M	$\langle v/c \rangle$
465.	26.	0.56	0.37

Table 3 - Compression modulus K, volume symmetry energy coefficient a_4, effective mass M^*/M and mean velocity $\langle v/c \rangle$ in nuclear matter, in DHF.

	^{16}O			^{40}Ca			^{48}Ca			^{90}Zr		^{208}Pb	
	-E/A	r_c	Δ_{LS}	-E/A	r_c	Δ_{LS}	-E/A	r_c	Δ_{LS}	-E/A	r_c	-E/A	r_c
DHF	5.61	2.73	7.3	6.62	3.47	6.0	7.10	3.47	4.1	7.40	4.26	6.74	5.47
Exp	7.96	2.73	6.3	8.55	3.46	7.2	8.67	3.47	4.3	8.71	4.27	7.87	5.50
CM	0.61			0.20			0.16			0.08		0.02	

Table 4 - Comparison betwen DHF and experimental values for finite nuclei. The non-relativistic center-of-mass corrections are indicated in line CM. Proton spin-orbit splittings for 1p shell(^{16}O) or 1d shell (^{40}Ca and ^{48}Ca) are shown. Energies are in MeV, radii in fm.

Meson	σ	ω	π	ρ	η	δ
Mass (MeV)	571.	764.	139.	764.	550.	962.
Set(B) $g^2/4\pi$	7.8	11.7	14.16	0.43	2.0	1.43
Set(B) f/g		0.		5.1		
Set(C) $g^2/4\pi$	6.4	11.7	14.16	0.43	2.0	0.
Set(C) f/g		0.		4.9		
Set(C) $f^2_{N\Delta}/4\pi$			0.35	4.0		

Table 5 - Parameters of OBE interaction. Set (B) is without Δ , set (C) with Δ degree of freedom.

A	Orbital	Schmidt	Valence	Valence core	Exp
15	$1p_{1/2}$	0.167	0.343	0.190	0.216
17	$1d_{5/2}$	1.440	1.570	1.430	1.414
39	$1d_{3/2}$	0.636	1.015	0.640	0.706
41	$1f_{7/2}$	1.940	2.253	1.940	1.916

Table 6 - Comparison of isoscalar magnetic moments (adopted from ref.[11]).

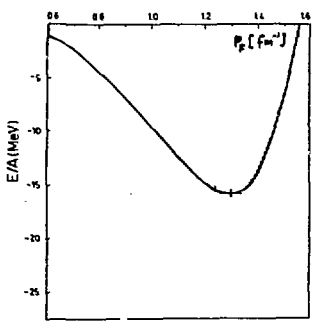

Fig.1 Binding energy per particle in nuclear matter (DHF).

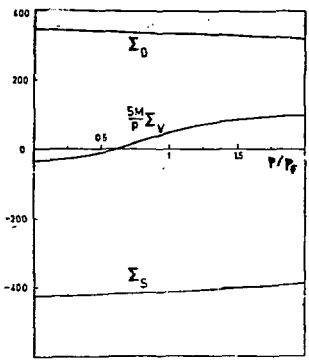

Fig.2 Self-energy components in nuclear matter (DHF).

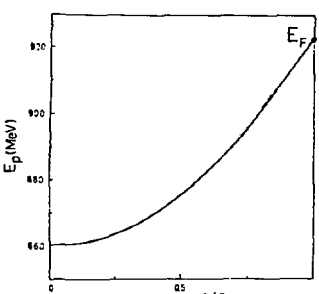

Fig.3 Single particle spectrum in nuclear matter (DHF).

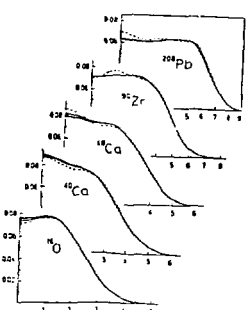

Fig.4 Calculated (dashed lines) and experimental [4D] (solid lines) charge distributions. Shaded areas correspond to experimental uncertainties.

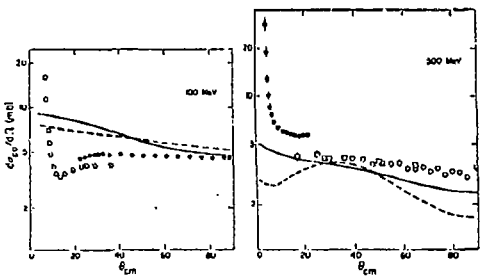

Fig.5 Differential p-p cross-sections at E_{lab} = 100 and 500 MeV. Solid and dashed curves correspond respectively to calculations with and without Δ .

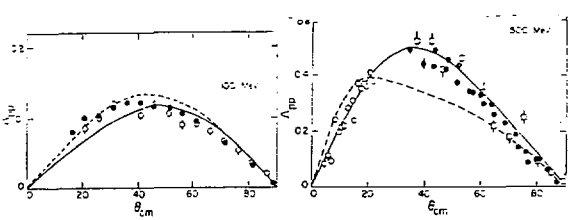

Fig.6 p-p polarization at E_{lab} = 100 and 500 MeV. The curves have the same meaning as in Fig.5.

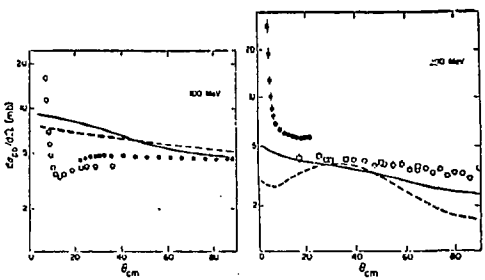

Fig.5 Differential p-p cross-sections at E_{lab} = 100 and 500 MeV. Solid and dashed curves correspond respectively to calculations with and without Δ.

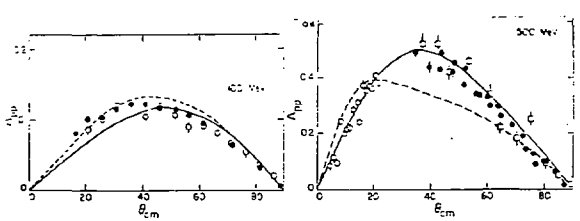

Fig.6 p-p polarization at E_{lab} = 400 and 500 MeV. The curves have the same meaning as in Fig.5.

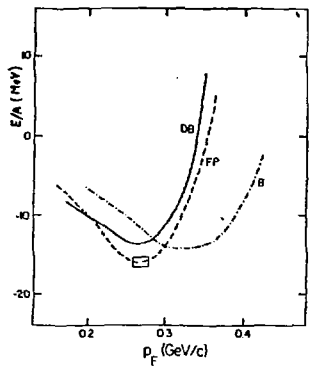

Fig.7 Saturation curve calculated in DB approach. The curves B and FP are explained in the text.

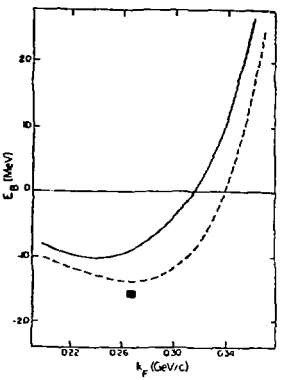

Fig.6 Saturation curves calculated in the DB approach, with Δ (solid line) and without Δ (dashed line).

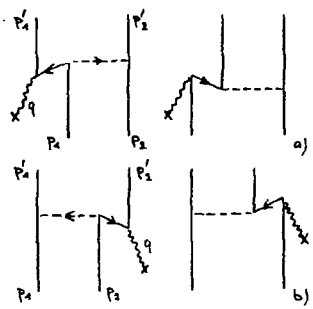

Fig.9 Exchange current contributions. Particle 1 is a valence nucleon whereas particle 2 is in the core. (a) : valence contributions; (b) : core contributions. Both processes (a) and (b) are necessary to insure gauge invariance. Note that (b) is the lowest order of RRPA.

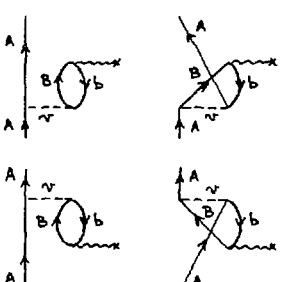

Fig.10 Lowest order RPA contributions to the current.

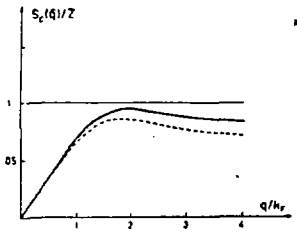

Fig.11 The sum rule $S_c^F(\vec{q})$ calculated with $M^*/M = 1$ (solid curve) and 0.56 (dashed curve) for $k_F = 1.42$ fm^{-1}.

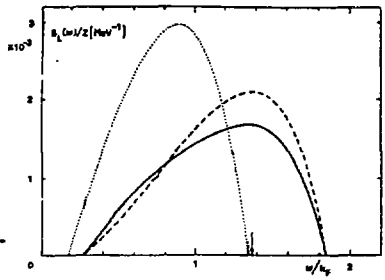

Fig 12 The longitudinal response for the momentum transfer $|\vec{q}| = 2.5\ k_F$. The curves correspond to a non-relativistic Fermi gas (dotted), Dirac-Hartree (dashed), RRPA (solid).

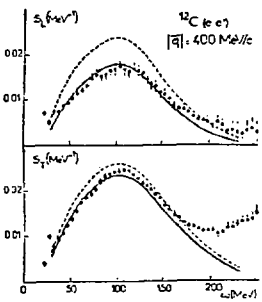

Fig.13 Calculated longitudinal and transverse responses. The solid curve is the relativistic calculation up to order $\vec{p}^2/M^{*2}$, the dashed curve is the conventional result. The data are from ref.[31].